ACR No. 3F26

NATIONAL ADVISORY COMMITTEE FOR AERONAUTICS

WARTIME REPORT

ORIGINALLY ISSUED
June 1943 as
Advance Confidential Report 3F26

FLIGHT TESTS OF AN ALL-MOVABLE VERTICAL TAIL ON THE FAIRCHILD XR2K-1 AIRPLANE

By Harold F. Kleckner

Langley Memorial Aeronautical Laboratory
Langley Field, Va.

NACA

WASHINGTON

NATIONAL ADVISORY COMMITTEE FOR AERONAUTICS

ADVANCE CONFIDENTIAL REPORT

FLIGHT TESTS OF AN ALL-MOVABLE VERTICAL TAIL ON THE FAIRCHILD XR2K-1 AIRPLANE

By Harold F. Kleckner

SUMMARY

Flight tests have been completed of an all-movable vertical tail of reduced area on the Fairchild XR2K-1 airplane. Results are in general agreement with the results previously obtained with a larger all-movable tail. The range of practical hinge positions and flap-linkage ratios was explored in particular. It was found that restrictions to the rearward placement of the hinge were necessary to avoid small-amplitude snaking oscillations. Several advantages of the all-movable tail continue to be evident: greater effectiveness, predictable and easily adjustable hinge-moment characteristics, and rudder stalling delayed to larger angles of sideslip for an airplane with rudder-fixed weathercock stability.

INTRODUCTION

The theory of operation of an all-movable tail surface and the results of preliminary flight tests of an all-movable tail on the Fairchild XR2K-1 airplane are given in reference 1. The flight tests of the all-movable type vertical tail have been continued in order to study the effects of a marked reduction in the vertical-tail area with the same airplane.

The second tail was expected to decrease the directional stability of the airplane to the point where complete stalling of the all-movable tail would occur in sideslips and permit the study of its behavior under the stalled conditions. In addition to the study of the tail-stalling characteristics, a study was planned to determine, insofar as possible, the practical limits of hinge position and flap-linkage ratio. The present report describes the results of these tests. Subsequent

additional work was done in studying the small-amplitude rudder oscillations obtained under certain conditions, but detail results of these tests are not yet available.

SYMBOLS

It will be noted that the symbols used in reference 1 for flap deflection (i) and rudder deflection (δ) have been changed in this paper to the NACA standard notation δ_f and δ_r respectively.

$\bar{c}$	mean aerodynamic chord of tail, inches
c_d	section drag coefficient
c_l	section lift coefficient
$c_{m_{c/4}}$	section pitching-moment coefficient
C_h	rudder hinge-moment coefficient $\left(\frac{H}{qS_t\bar{c}}\right)$
C_L	rudder lift coefficient
h_α	distance between hinge point and aerodynamic center of all-movable tail, fraction $\bar{c}$
h_{δ_f}	distance between hinge point and center of pressure of lift due to flap deflection, fraction $\bar{c}$
H	rudder hinge-moment, inch-pounds
I_Z	moment of inertia about Z axis, slug feet^2
q	dynamic pressure at tail, pounds per square foot
q_o	free-stream dynamic pressure, pounds per square foot
$\dot{r}$	angular acceleration about Z axis, radians per second per second
R	Reynolds number

S_t conventional fin and rudder area, square feet; all-movable tail area, square feet

α_o section angle of attack, degrees

α_e effective angle of attack of tail, degrees

α_t angle of attack of vertical tail, degrees

$\partial\alpha_e/\partial\delta_f$ relative effectiveness of flap on all-movable tail

$\partial\alpha_e/\partial\delta_r$ relative rudder effectiveness

δ_f deflection of flap of all-movable tail, degrees

δ_r deflection of conventional rudder, degrees; deflection of all-movable tail, degrees

η rudder floating ratio $(C_{h_\alpha}/C_{h_{\delta_r}})$

$C_{L_{\delta_r}} = \partial C_L/\partial\delta_r$

$C_{L_\alpha} = \partial C_L/\partial\alpha_t$

$C_{h_{\delta_r}} = \partial C_h/\partial\delta_r$

$C_{h_\alpha} = \partial C_h/\partial\alpha_t$

TAIL CHARACTERISTICS

The second all-movable vertical tail (figs. 1 to 4) was similar to but was one-half the area of the tail surface described in reference 1. The characteristics of the second tail are as follows:

Fixed area (fuselage extension, fairing), square feet	1.3
Movable area (including flap area), square feet	5.8
Flap area (19 percent of movable area), square feet	1.1
Aspect ratio	2.9
Taper ratio	1.5:1
Mean aerodynamic chord, $\bar{c}$, inches	17.8
Airfoil section	NACA 65,3-018

The section characteristics of the NACA 65,3-018 airfoil are given in figures 5 and 6. Figure 5 is taken from reference 2. Figure 6 is from unpublished data taken in the NACA low-turbulence tunnel.

The tail was of wood construction, plywood covered, with ball bearings at the main hinge. Provision was made for hinging the tail at any point between $0.26\bar{c}$ and $0.36\bar{c}$. The flap was hinged at 80 percent of the airfoil chord and sealed with 0.008-inch sheet rubber. The method of actuating the flap was the same as that described in reference 1 with a wide range of deflection ratios δ_f/δ_r available. Incorporated in the second tail for trimming was a unit to change the initial setting of the flap.

During the course of the tests several minor modifications were made in the tail arrangement, as follows:

1. In order to reduce the control friction for rudder-free tests, the rudder cables were slacked and a bungee was used at each cable to keep the slack at the tail end of the system. The arrangement permitted the pilot to use the rudder, yet removed the friction of the pedal and cable system for approximately 8° of right and left rudder movement; the friction was thus reduced from about 30 inch-pounds to 5 inch-pounds (static moment about the rudder hinge line).

2. For two flights, weight was added forward of the hinge. This added weight changed the mass balance to about 50 inch-pounds of overbalance and put the center of gravity of the tail at $0.30\bar{c}$.

3. In order to obtain a small value of $C_{h_{\delta_f}}$ without using an excessively low flap-linkage ratio, a partial-span flap was used on the tail for one flight. The original flap (fig. 4(a)) was cut in two, and the upper half was fixed. (See figs. 3 and 4(b).) The characteristics of the tail in this revised form are as follows:

Flap span (46 percent of tail span), inches	23
Flap area (10 percent of movable area), square feet	0.6

TESTS

The tail configurations covered in the flight tests are summarized in table I.

Measurements were made with NACA recording instruments of indicated airspeed, yawing velocity, angle of sideslip, control position, and rudder force. The test data presented were obtained in the gliding condition, but in all cases tests were also made with power on. Runs were made at approximately 60 and 85 miles per hour indicated airspeed; corresponding Reynolds numbers for the tail were about 800,000 and 1,000,000, respectively.

The tests were of five types: steady sideslips, rudder "kicks," lateral oscillations, aileron rolls, and straight flight runs. For the sideslips and rudder kicks, a flap-linkage ratio δ_f/δ_r of 2.2 was used. The value of the linkage ratio taken is the slope through zero of the curve of the variation of flap deflection with main surface deflection, and the value 2.2 is the linkage ratio used with the first all-movable tail. (See fig. 16, reference 1.) The sideslip records were obtained as the sideslip was slowly increased from zero to the maximum. The rudder kicks involved abrupt rudder deflection with the stick held fixed in the trim position.

The lateral oscillations were of two types. One type was started by applying and releasing the rudder with the stick held fixed. The second type was made with the rudder free by abruptly applying the aileron control.

Aileron rolls were made to investigate the directional stability and tail stalling characteristics. The maneuver consisted of applying abrupt aileron deflection to the limit of a "stop" and holding that deflection until the maximum angle of sideslip was obtained. The amount of aileron deflection was limited to give reasonable amounts of sideslip. The aileron rolls and lateral oscillations were made with various flap-linkage ratios and tail hinge positions.

Records of straight flight were made in flights 8 and 13 to obtain hinge-moment and flap-effectiveness data.

RESULTS AND DISCUSSIONS

Rudder effectiveness.- The maximum yawing velocities and accelerations obtained with rudder deflection in the rudder kick tests are presented in figure 7. The values of yawing acceleration were obtained by differentiating the records of yawing velocity. To the table of reference 1, which is repeated herein, is added the rudder effectiveness as determined for the second tail:

Tail	I_Z	S_t	$\frac{q}{q_o}$	q_o	$\frac{\partial \dot{r}}{\partial \delta_r}$	$C_{L_{\delta_r}}$	C_{L_α}
Original	1660	13.7	0.80	9.3	0.025	0.027	0.034
Large all-movable tail of reference 1	2080	11.6	.85	10.0	.050	.075	.045
Second all-movable tail	1890	5.8	.80	10.0	.029	.079	.042

Included in the effectiveness of the all-movable tail is the effectiveness of its flap. For the first all-movable tail, a value of 0.3 was assumed for $\partial\alpha_e/\partial\delta_f$; for the second tail (sealed flap), tests indicated a value of 0.4.

Directional stability.- The variation of rudder angle with angle of sideslip obtained in the steady sideslips is presented in figure 8 together with similar results from reference 1. The directional stability measured in this way was not materially reduced by the change to the small tail. Evidently the airplane is about neutrally stable directionally with the tail off.

The extent to which the positive floating ability of the tail increased the control-free directional stability was investigated in abrupt aileron rolls. The results given in figure 9 show the sideslip obtained with 12° total aileron deflection for various rudder floating ratios. The floating ratio $\eta = C_{h_\alpha}/C_{h_{\delta_r}}$ is negative because C_{h_α} is positive and $C_{h_{\delta_r}}$ is negative. The term positive floating tendency arises from the fact that

C_{h_α} is positive. A positive floating tendency gives a negative floating ratio. The method of obtaining the floating ratio is discussed subsequently. Curves are also shown in figure 9 of the sideslip that could be expected theoretically. It is apparent that the floating ability of the rudder reduced the angle of sideslip, but this reduction was not as great as was expected. The principal reason appears in the time histories (fig. 10) of a typical aileron roll and a small amplitude oscillation made in flight 11 with the tail hinged at $0.30\bar{c}$ and a flap-linkage ratio of 2.35. The floating ratio obtained for small angles of sideslip was not maintained for large angles.

Rudder-free lateral motion.- The lateral oscillation produced by deflecting the rudder and releasing it at an angle of sideslip is the type from which the buffeting oscillation mentioned in reference 1 can be obtained. With the second tail, buffeting was obtained with low as well as with high floating ratios if the rudder was released at a sufficiently large angle of sideslip. The tests confirm the opinion that the oscillation is not particularly objectionable because it cannot be produced except by this maneuver.

In flight 6 with the hinge at 32 percent $\bar{c}$ and a 1.9 linkage ratio, a continuous yawing oscillation (snaking) of about 1° was obtained with the rudder free. This snaking is the oscillation mentioned in reference 1 that sometimes occurs with a rudder having positive C_{h_α} and friction. Inasmuch as the all-movable tail installation afforded a ready means of independently adjusting C_{h_α} and $C_{h_{\delta_r}}$, an additional series of tests (flights 7 to 19) were made to study the snaking problem. The complete results of the additional tests are not yet available; however, the immediate results are given in the following table which lists the configurations from which snaking resulted.

Flight	Hinge position (percent $\bar{c}$)	Flap-linkage ratio, δ_f/δ_r	Approximate friction (in.-lb)
6	32	1.9	5
10	30	1.05	20
12	30	1.7	5
[a]14	30	1.7	5
[b]19	26	1.5	5

[a]Rudder mass overbalanced about 50 inch-pounds.
[b]Half-span flap.

The magnitude of the oscillations was less than 1.5° except in flight 10, when it was about 6°.

The test results indicated that hinge positions and flap-linkage ratios that gave a value of $\frac{\partial \alpha_e}{\partial \delta_r} \times \frac{C_{h_\alpha}}{C_{h_{\delta_r}}} \leq 0.7$ could be used with the second all-movable tail without experiencing snaking. However, some normal lateral oscillations of the airplane that were produced with about this value of $\frac{\partial \alpha_e}{\partial \delta_r} \times \frac{C_{h_\alpha}}{C_{h_{\delta_r}}}$ did not satisfy the requirement of reference 3, that the oscillation should damp to one-half amplitude in two cycles. A second requirement of reference 3, that any oscillation of the rudder shall have disappeared after one cycle, was not satisfied when the rudder was given a high floating ratio. In the present tests no particularly undesirable effects were noted when oscillations of the rudder continued after one cycle if the oscillation of the airplane was satisfactorily damped. Tests were made, however, only in smooth air conditions.

Tail stalling.- Partial stalling of the tail was obtained in steady sideslips. Complete stalling of the tail was obtained in rudder kicks from a sideslip and with rudder free in aileron rolls. No adverse effects were encountered. A time history of a typical aileron roll made with rudder free in which the tail stall occurred is presented in figure 11. The record shows that the rudder started to float against the sideslip, stalled

at about $2\frac{3}{4}$ seconds, and remained stalled near neutral as the sideslip passed a maximum. The pilot resumed control at about $5\frac{1}{2}$ seconds. There is no evident tendency for the rudder to start oscillating between the stalled and the unstalled conditions as it does when released in a sideslip.

Rudder hinge moments.- It is apparent that a wide range of rudder force characteristics can be obtained by variations in the tail hinge position and flap-linkage ratio. An attempt has been made to correlate values of hinge moments calculated by means of simplified formulas with the hinge moments measured in flights 8 and 13, which were straight flight runs with various trim settings (various values of α_t and δ_r).

It is convenient to consider the hinge moments in terms of the lift or normal force acting on the tail. If the lift due to angle of attack of the tail acts at the aerodynamic center and the lift due to flap deflection acts at some fixed point, the following relations are apparent:

$$H = q_o \frac{q}{q_o} S_t \bar{c} C_{L_\alpha} \left(\alpha_t h_\alpha + \frac{\partial \alpha_e}{\partial \delta_f} \delta_f h_{\delta_f} \right) \qquad (1)$$

$$C_{h_\alpha} = C_{L_\alpha} h_\alpha \qquad (2)$$

$$C_{h_{\delta_r}} = C_{L_\alpha} \left(h_\alpha - \frac{\delta_f}{\delta_r} \frac{\partial \alpha_e}{\partial \delta_f} h_{\delta_f} \right) \qquad (3)$$

$$\text{Floating ratio} = \eta = \frac{C_{h_\alpha}}{C_{h_{\delta_r}}} = \frac{h_\alpha}{h_\alpha - \frac{\delta_f}{\delta_r} \frac{\partial \alpha_e}{\partial \delta_f} h_{\delta_f}} \qquad (4)$$

In these relations the contribution of the flap hinge moment about its own hinge is neglected.

The floating ratios obtained with equation (4) were in agreement with those indicated in the rudder-free oscillations when the aerodynamic center was assumed to be at $0.25\bar{c}$ and the center of pressure of the lift due to flap deflection was assumed to be $0.50\bar{c}$. It follows then that

$$h_{\alpha} = (\text{hinge position} - 0.23\bar{c}) \qquad (5)$$

$$h_{\delta_f} = (0.50\bar{c} - \text{hinge position}) \qquad (6)$$

where the hinge position is in chord lengths back of the leading edge.

For the first hinge-moment calculations, values of $q/q_o = 0.8$ and $C_{L_\alpha} = 0.042$ obtained from the rudder-effectiveness calculations were used in equation (1). A comparison with the measured values is given in figure 12(a) in which the calculated values are seen to be lower than the measured values. Better agreement was obtained when it was assumed that $q/q_o = 0.9$ and, from figure 3 of reference 4, $C_{L_\alpha} = 0.53$ for a tail aspect ratio of 2.9 if the gap at the bottom of the tail was assumed to eliminate any end-plate effect from the horizontal tail. The correlation for this case is shown in figure 12(b). The results indicate that hinge moments for the all-movable tail can be predicted with sufficient accuracy for the present by the simple relations established above.

The values of C_{L_α} indicated by the yawing accelerations are lower than those indicated by the hinge-moment analysis and by reference 4. The most logical explanation for the disagreement appears to be the experimental error in the determination of yawing accelerations.

Future research.- The all-movable tail continues to show promise as a means of improving the directional control of aircraft. The greater effectiveness of the tail may permit some reduction in the size of tail surfaces. If sufficient tail area is used to give rudder-fixed, weathercock stability, the all-movable tail will increase the angle of sideslip at which tail stalling occurs. The availability of hinge-moment adjustment by means of the hinge location and the flap-linkage ratio offers the opportunity to obtain reduced rudder forces.

It is planned to continue the research with tests of an all-movable vertical tail on a pursuit-type airplane.

CONCLUSIONS

From the results of flight tests of an all-movable vertical tail of 5.8 square feet area on the Fairchild XR2K-1 airplane, the following observations can be made:

1. The tail characteristics were considered satisfactory over a normal range of hinge positions and flap-linkage ratios.

2. The floating ratio of the tail was lower at large angles of sideslip than at small angles; as a result, the increase in directional stability with rudder free was not as great as was expected.

3. Close control over the floating ratio of the tail was necessary in order to avoid continuous yawing oscillations of small amplitude (snaking) and to insure satisfactory damping and rudder movement in rudder-free lateral oscillations.

4. Stalling of the tail was obtained in rudder kicks and aileron rolls and was apparent to the pilot only through observation of tuft action on the tail. Complete stalling was not obtained in steady sideslips as the sideslip angles obtainable with full rudder were insufficient to stall the tail.

5. Measured hinge moments were in agreement with hinge moments calculated by simplified relations based on the lift acting on the surface.

Langley Memorial Aeronautical Laboratory,
National Advisory Committee for Aeronautics,
Langley Field, Va.

REFERENCES

1. Jones, Robert T., and Kleckner, Harold F.: Theory and Preliminary Flight Tests of an All-Movable Vertical Tail Surface. NACA A.R.R., Jan. 1945.

2. Jacobs, Eastman N., Abbott, Ira H., and Davidson, Milton: Supplement to NACA Advance Confidential Report, Preliminary Low-Drag-Airfoil and Flap Data from Tests at Large Reynolds Numbers and Low Turbulence. NACA, (Loose leaf), March 1942.

3. Gilruth, R. R.: Requirements for Satisfactory Flying Qualities of Airplanes. NACA A.C.R., April 1941.

4. Pass, H. R.: Analysis of Wind-Tunnel Data on Directional Stability and Control. T.N. No. 775, NACA, 1940.

TABLE I

RÉSUMÉ OF TESTS

Flight	Hinge position (percent $\overline{c}$)	Flap linkage ratio, δ_f/δ_r	Approximate friction (in.-lb)
1	27	1.5	20
2	27	1.5	20
3	27	2.2	20
4	30	2.2	20
5	30	2.2	5
6	32	1.9	5
7	32	3.9	5
8	27	2.0	20
9	30	2.35	20
10	30	1.05	20
11	30	2.35	5
13	30	1.7	5
[a]13	30	1.7	20
[a]14	30	1.7	5
15	30	3.3	5
16	30	3.3	10
17	30	1.5	5
18	27	1.0	5
[b]19	26	1.5	5

[a]Rudder mass over-balanced.
[b]Half-span flap.

Figure 1.- Second all-movable vertical tail on Fairchild XR2K-1 airplane.

L-397

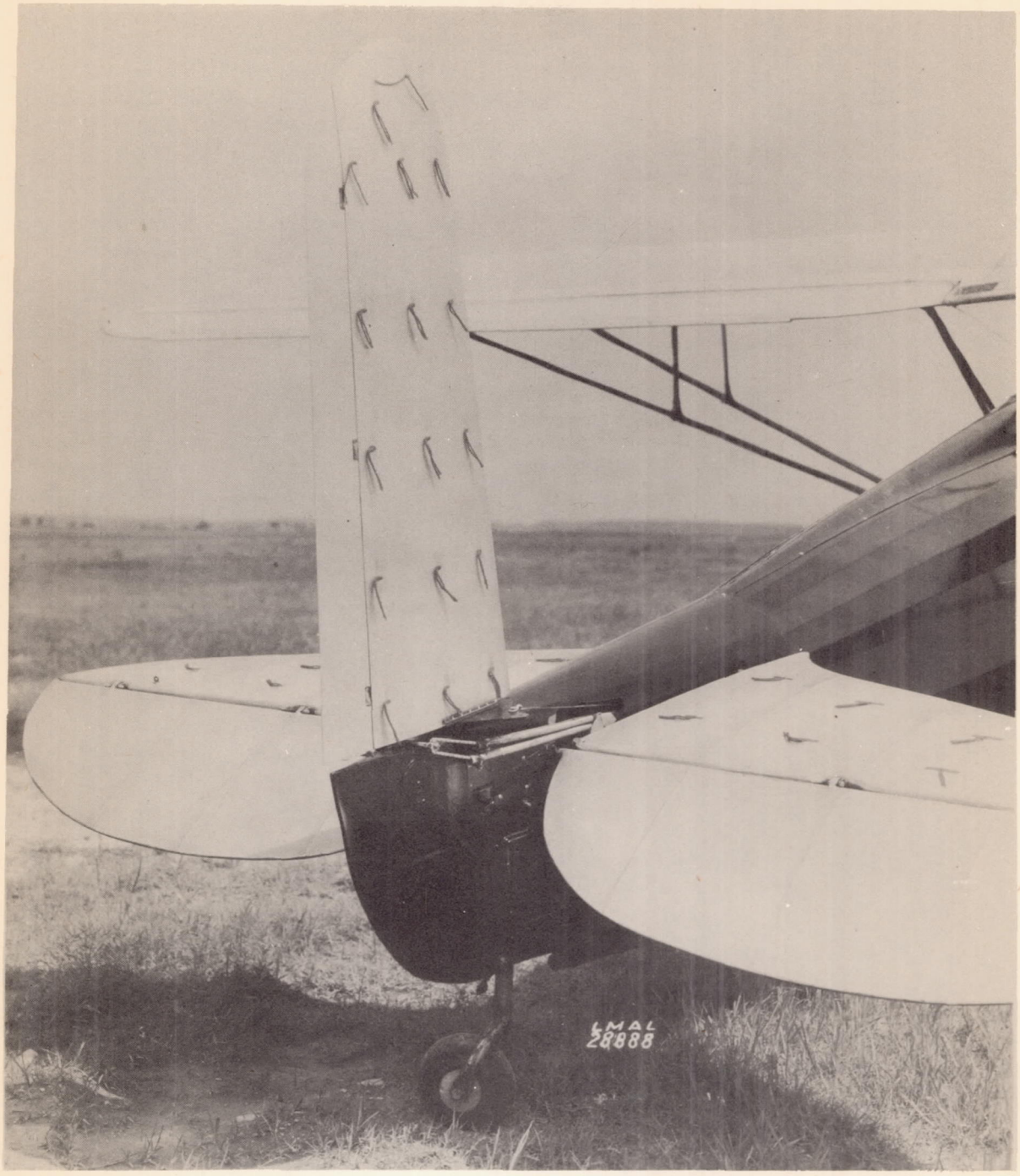

Figure 2.- Second all-movable vertical tail with full-span flap

L-67

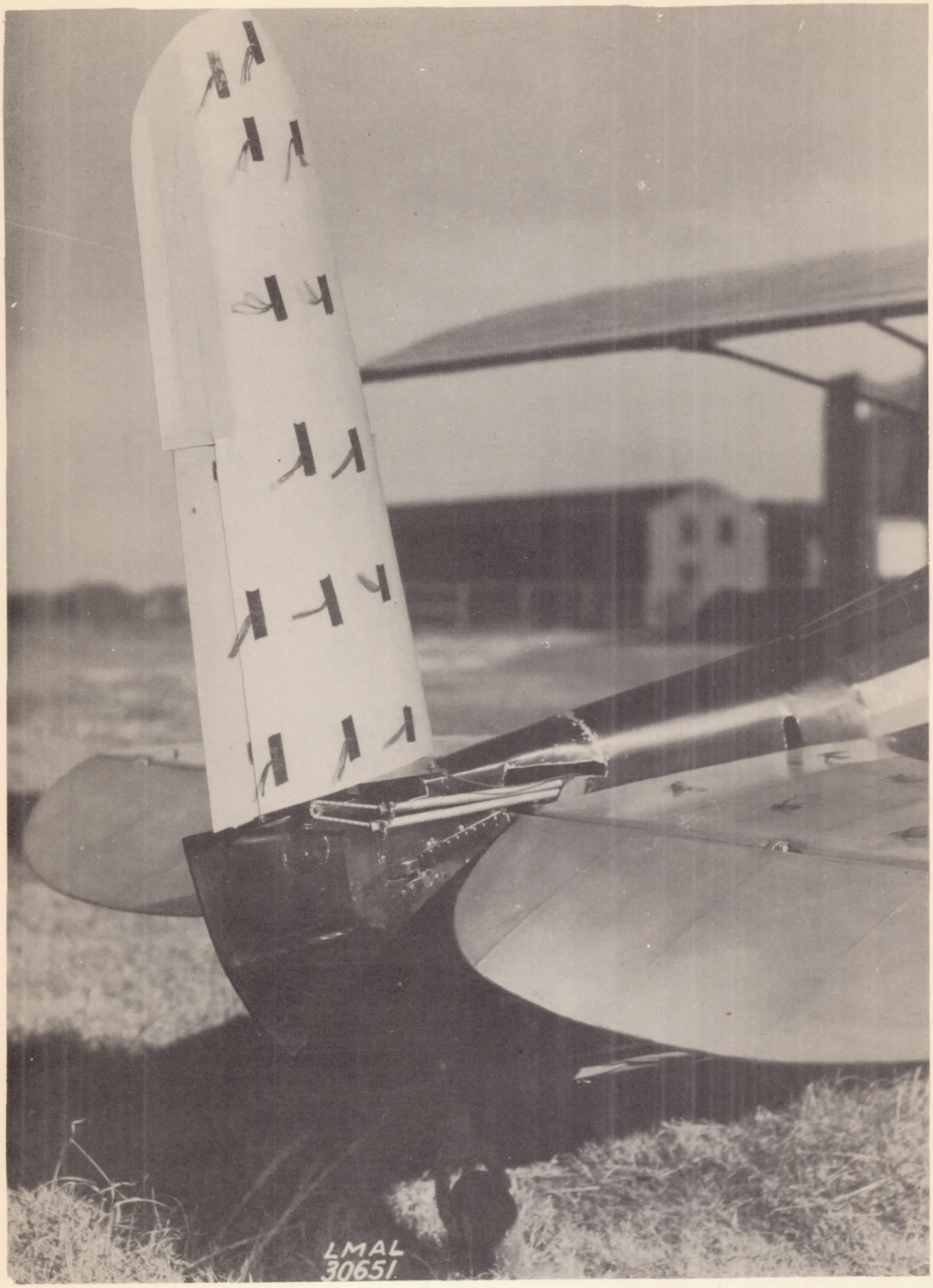

Figure 3.- Second all-movable vertical tail with half-span flap.

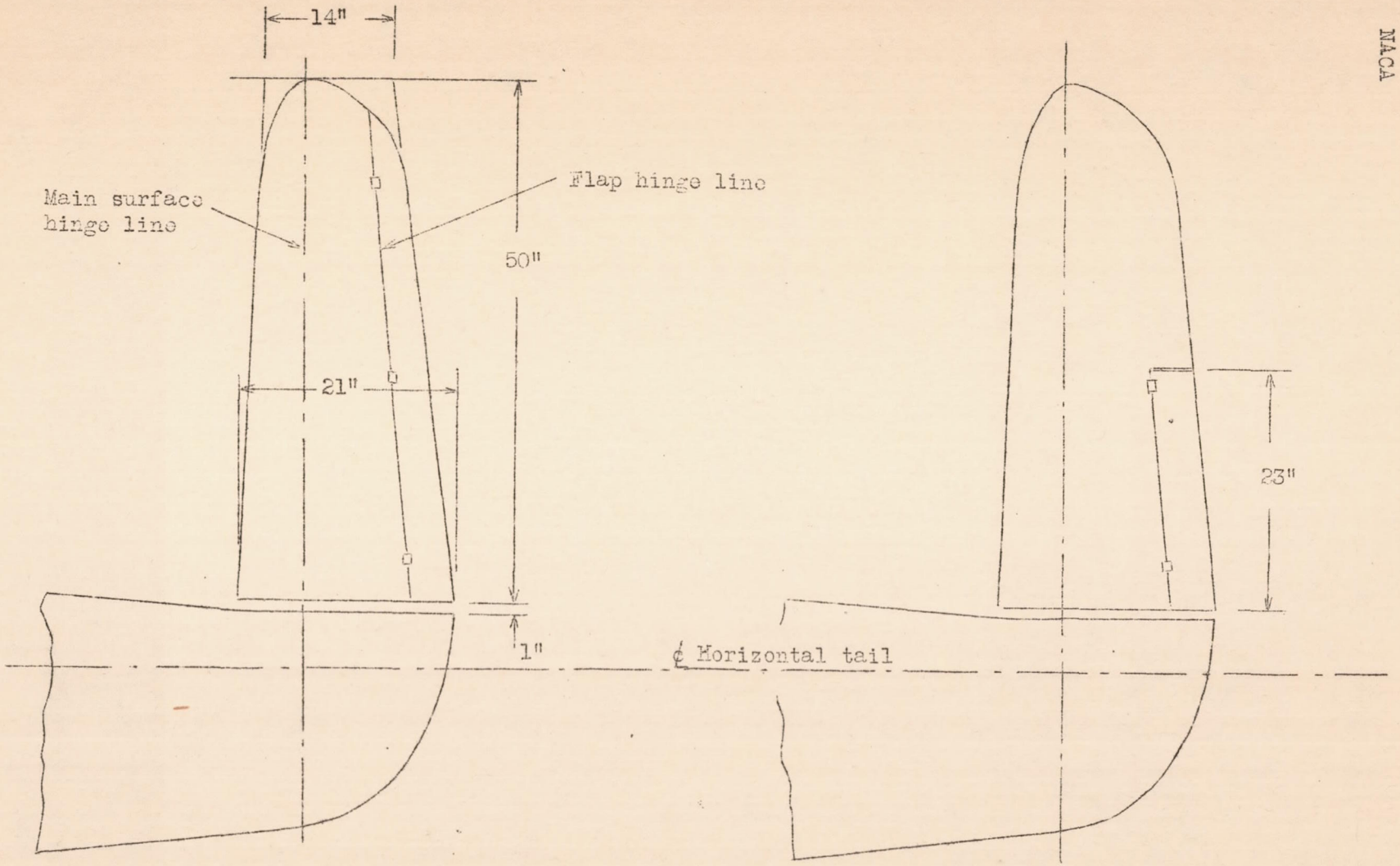

(a) Full-span flap

(b) Half-span flap

Figure 4.- Second all-movable vertical tail for Fairchild XR2K-1 airplane.

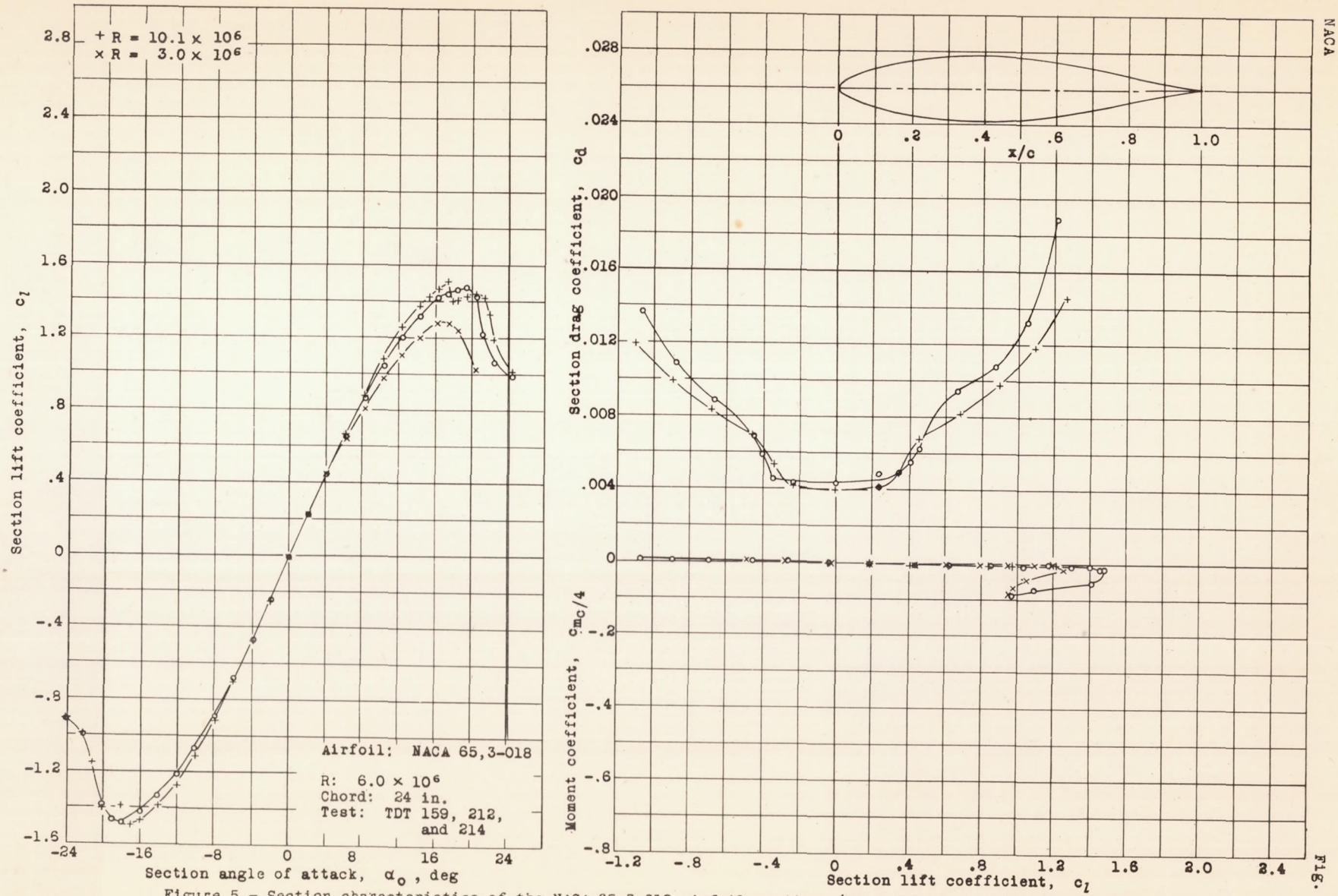

Figure 5.- Section characteristics of the NACA 65,3-018 airfoil section. (This figure is taken from reference 2. The symbol o is for values at which R = 6 × 10⁶.)

Fig. 5

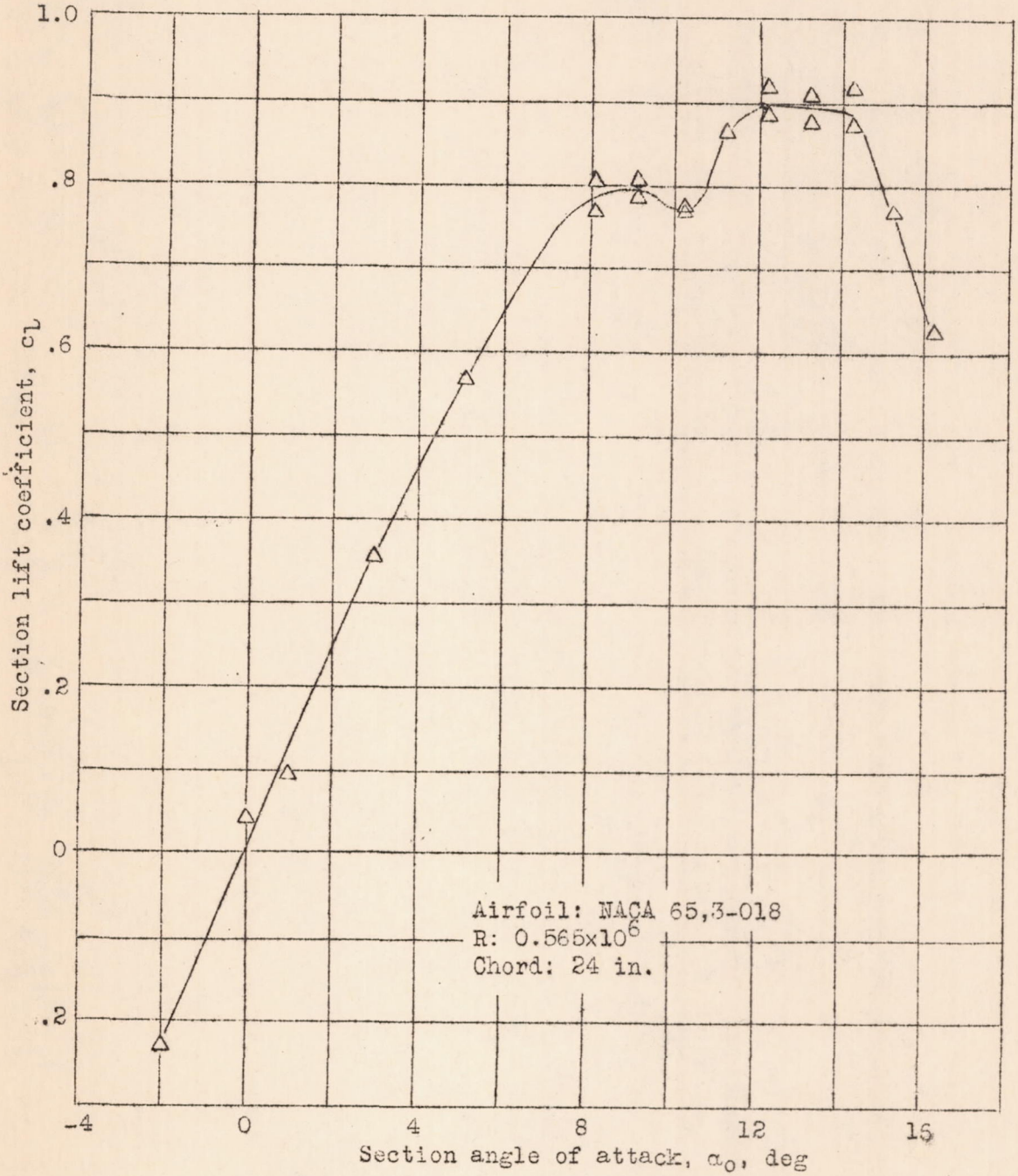

Figure 6.- Section lift characteristics of the NACA 65,3-018 airfoil section at low Reynolds number. Data from NACA two-dimensional low-turbulence tunnel.

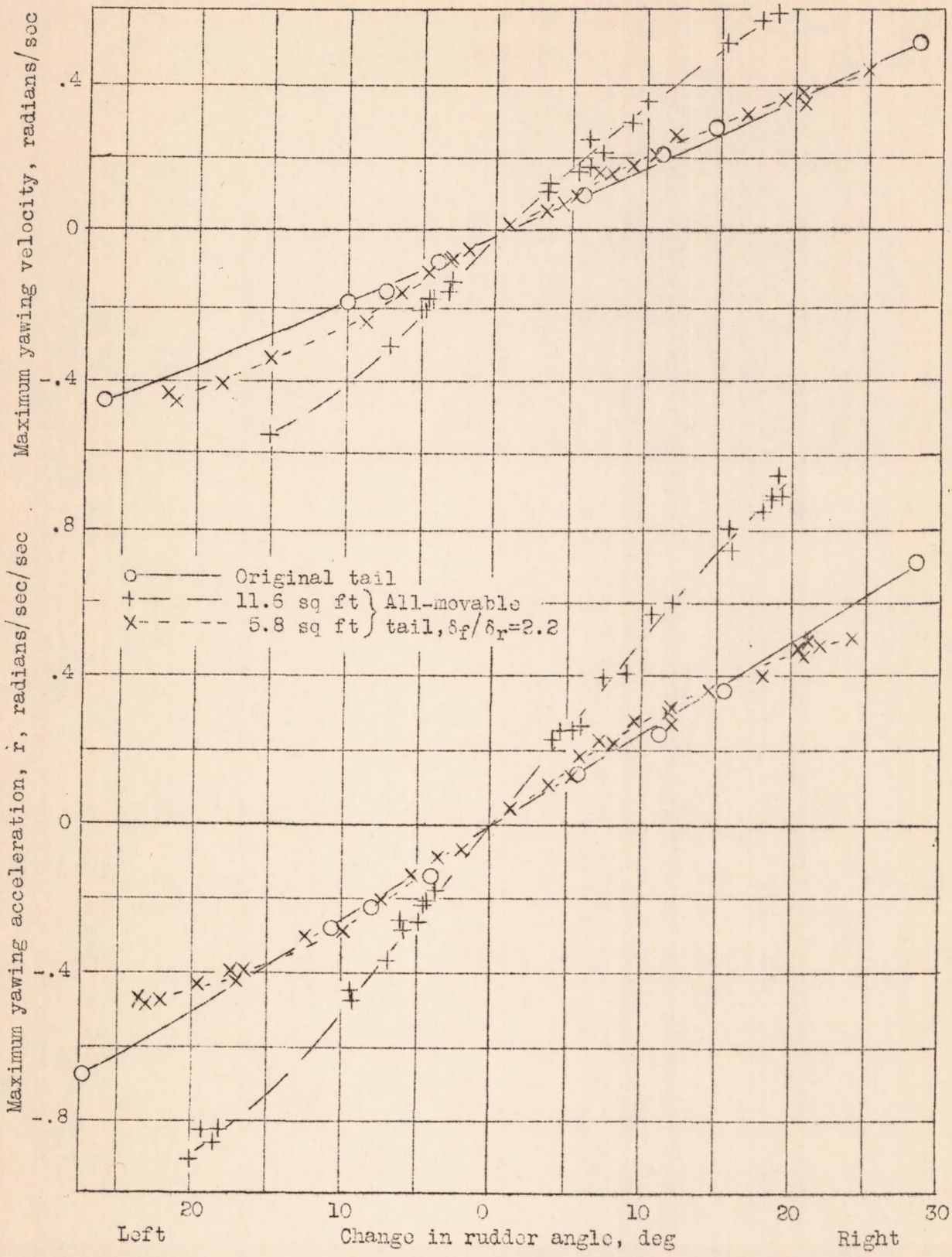

Figure 7.- Variation of maximum yawing acceleration and maximum yawing velocity with change in rudder angle. Abrupt rudder deflection with Fairchild XR2K-1 airplane at 60 mph in the gliding condition.

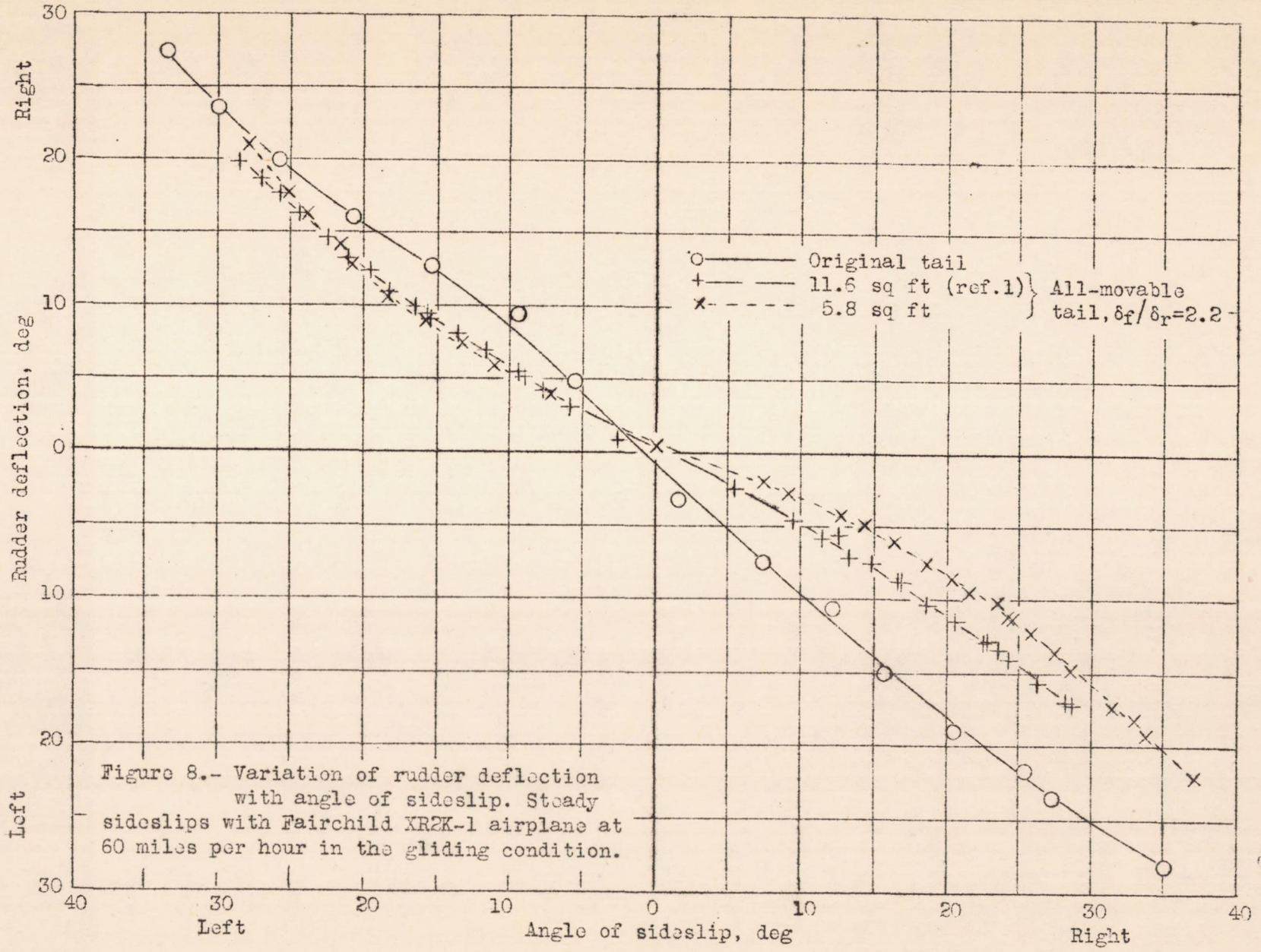

Figure 8.- Variation of rudder deflection with angle of sideslip. Steady sideslips with Fairchild XR2K-1 airplane at 60 miles per hour in the gliding condition.

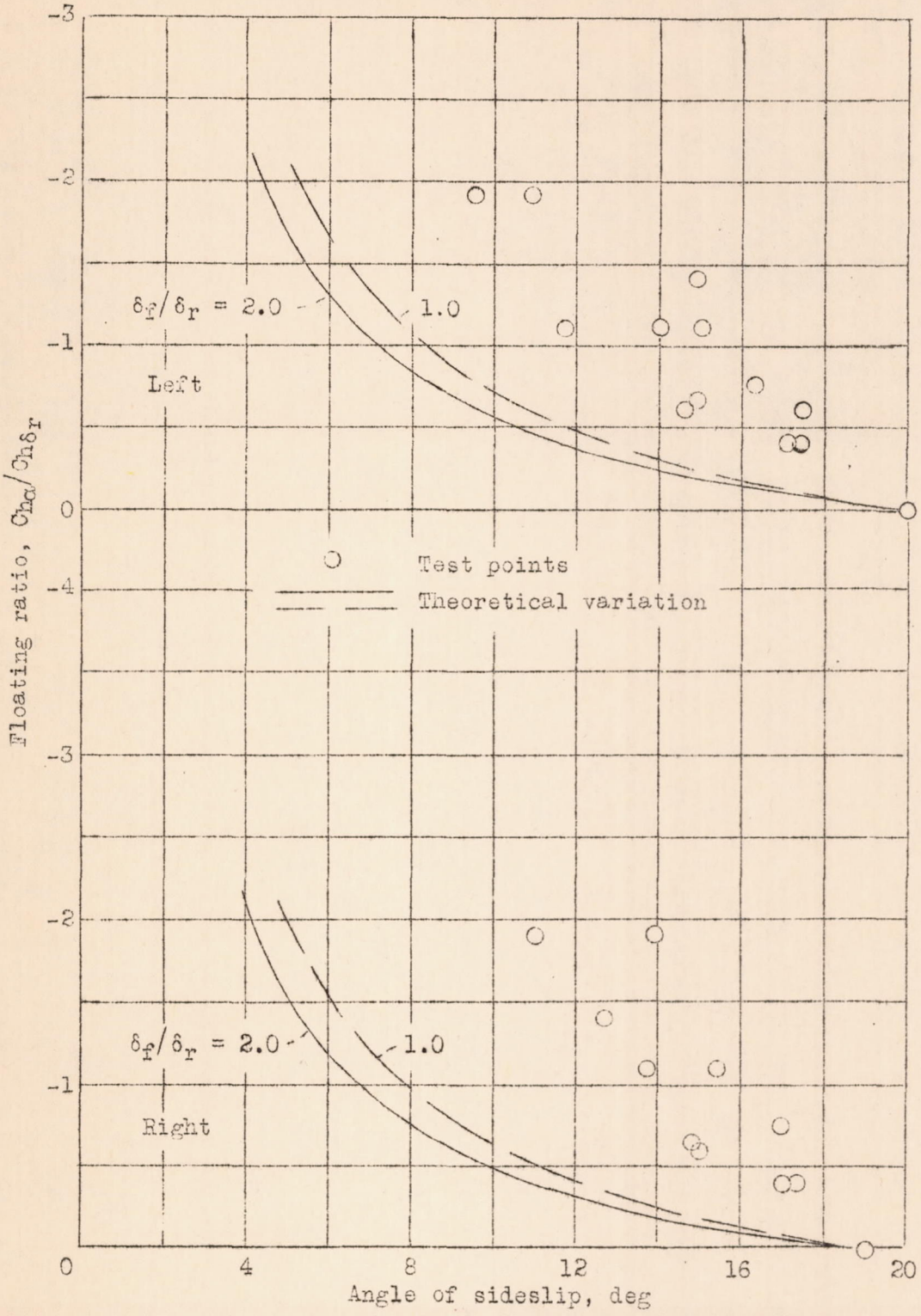

Figure 9.- Variation with rudder floating ratio of the angle of sideslip obtained in aileron rolls of 12° total aileron deflection. Fairchild XR2K-1 airplane with all-movable vertical tail area of 5.8 square feet.

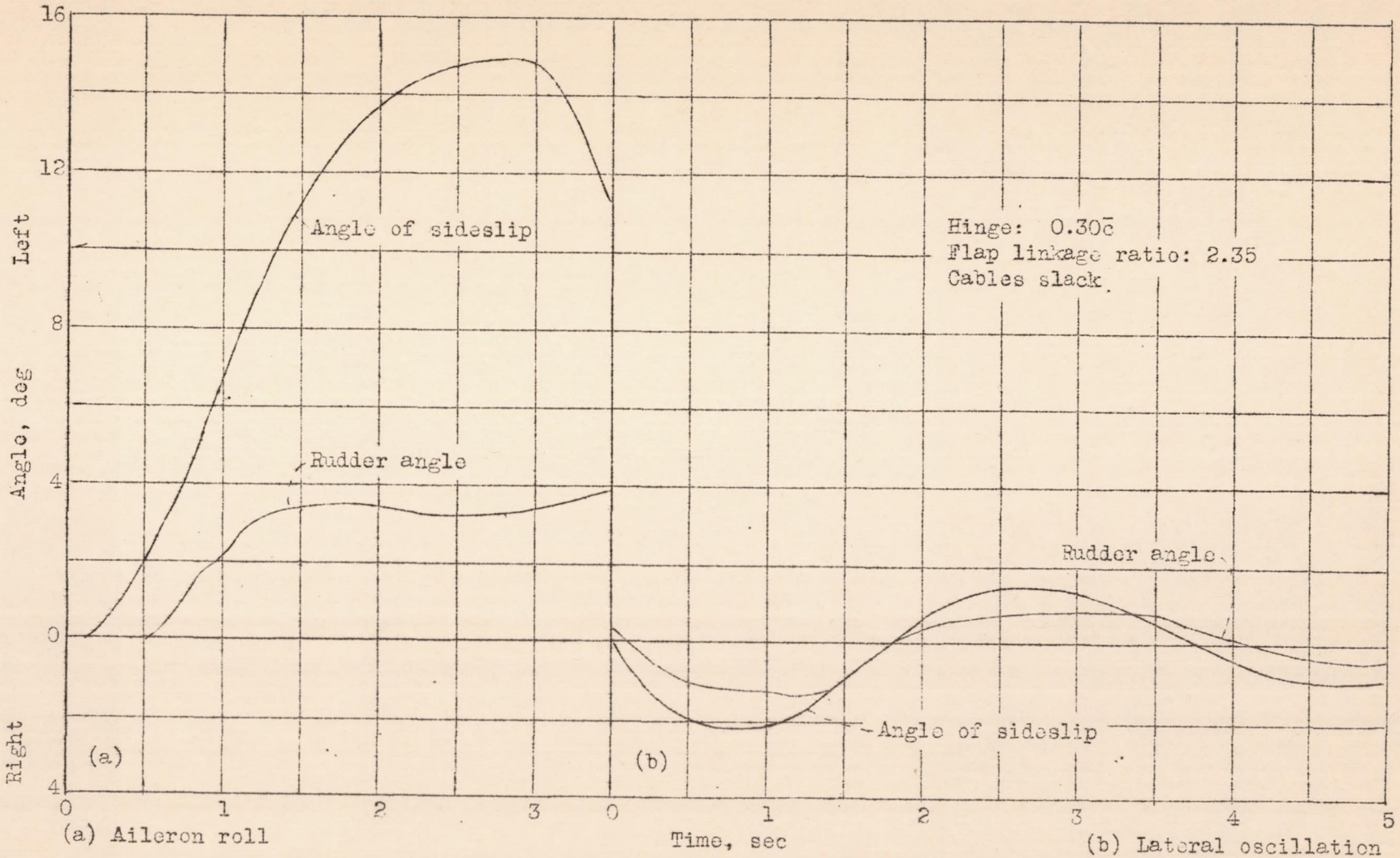

Figure 10.- Time histories of an aileron roll and a lateral oscillation. Fairchild XR2K-1 airplane with all-movable vertical tail area of 5.8 square feet.

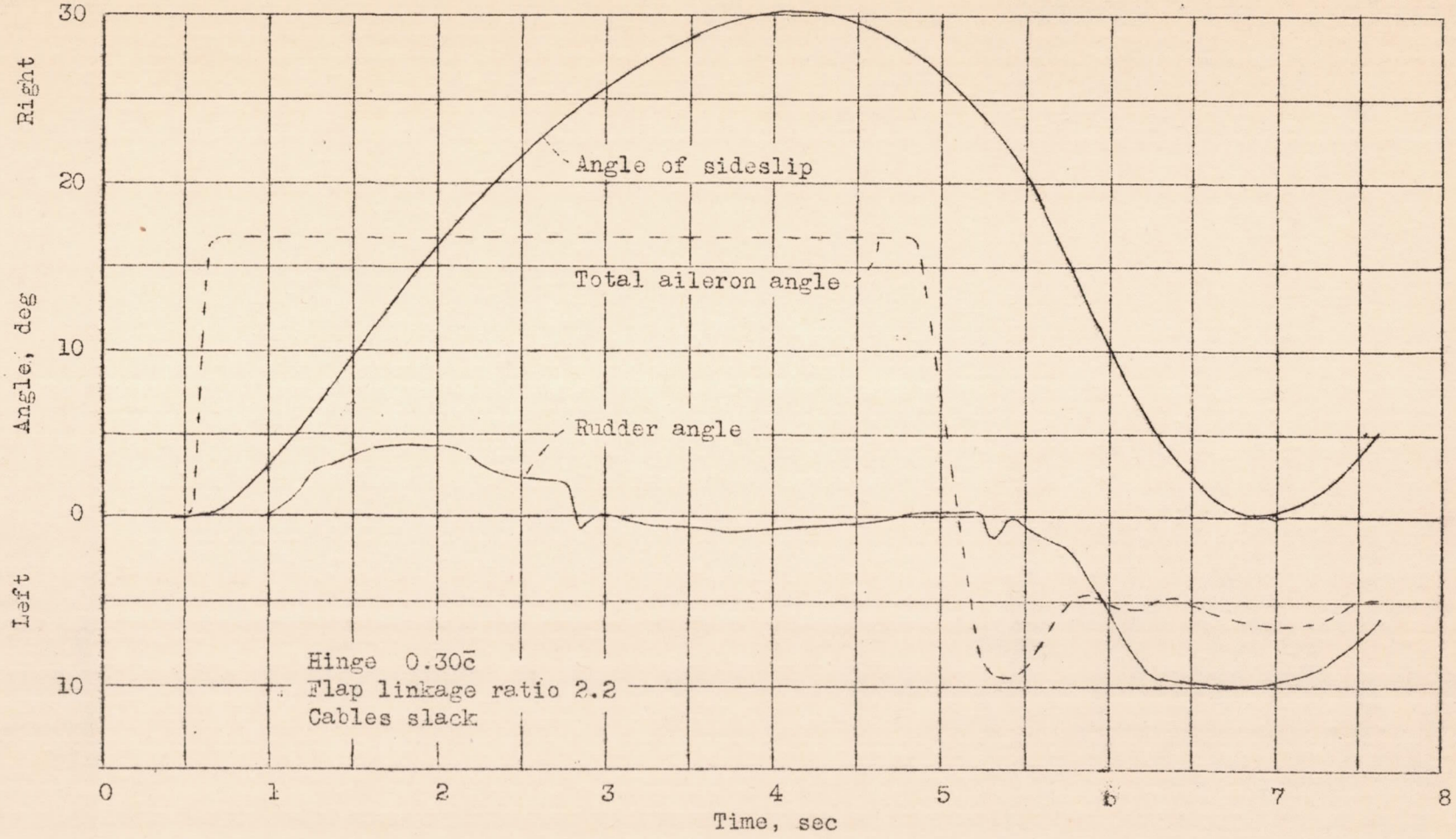

Figure 11.- Time history of an abrupt aileron roll. Fairchild XR2K-1 airplane with all-movable vertical tail area of 5.8 square feet.

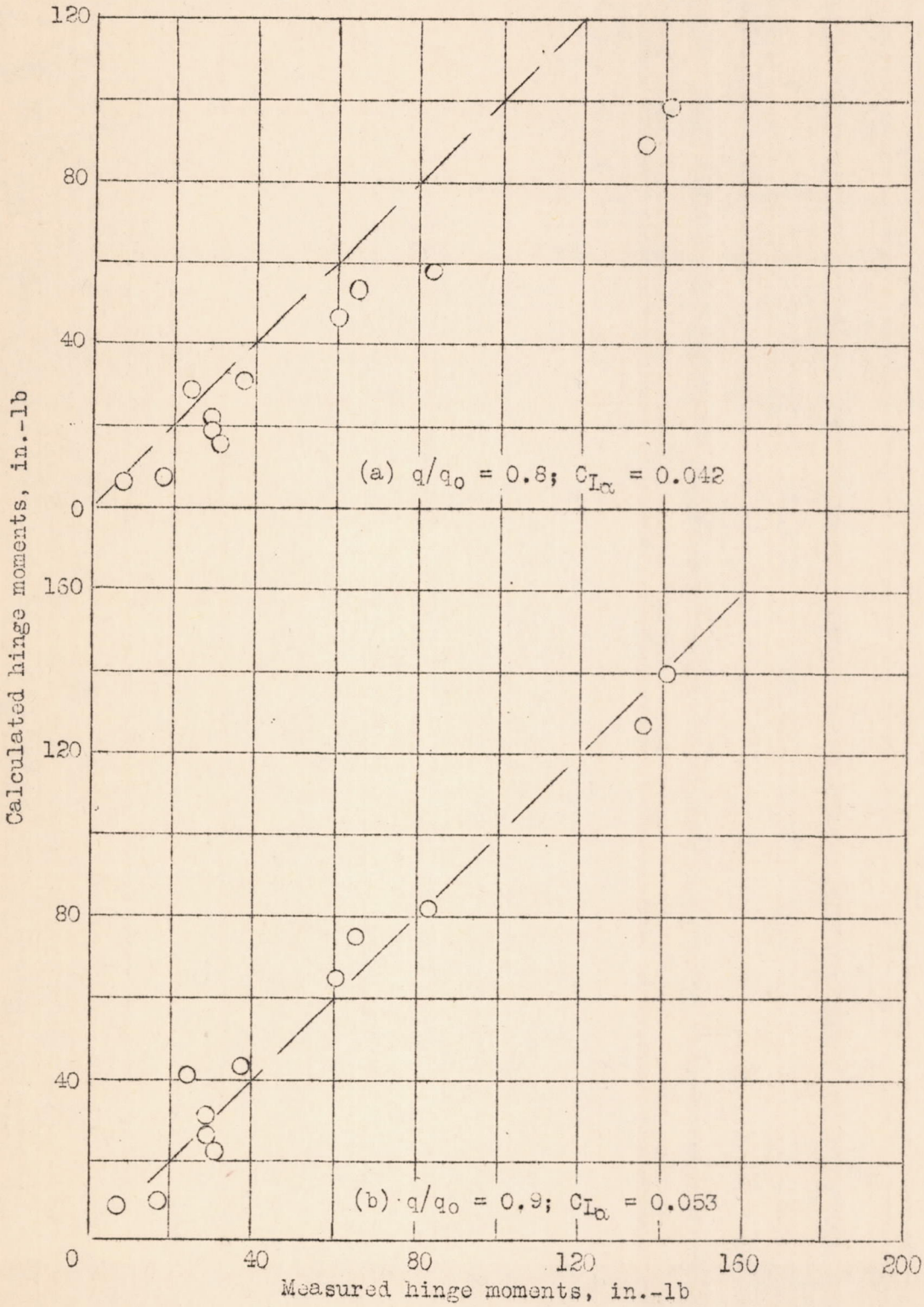

Figure 12.- Correlation of measured and calculated hinge moments.